ISSN: 2688-8645

Experimental Study on the Clamping Performance of Worn Snubbing Unit Slips

Lin Zhong [1, 2], Xulong He [1, 2], Dan Zhu [1, 2], Guorong Wang [1, 2], Yang Wang [1, 2], Chuan Wang [1, 2], Miao He [1, 2]

[1] School of Mechatronic Engineering, Southwest Petroleum University, Chengdu, Sichuan 610500, China

[2] Energy Equipment Institute, Southwest Petroleum University, Chengdu, Sichuan, 610500, China

Abstract

The height of the slip teeth directly affects the gripping efficiency of Snubbing Units. However, there is currently a lack of experimental methods for quantitatively assessing the height of worn slip teeth and their gripping capability. Therefore, a die-cutting inspection method was adopted to measure worn slip heights quantitatively. An experimental platform was developed to simulate the actual loading conditions of Snubbing Units during pipe-to-pipe gripping. Using image processing techniques based on pressure-sensitive paper color changes and grayscale values, experiments were conducted to evaluate the pipe-gripping performance of slips with varying wear heights under simulated operational conditions. By applying the least squares method to fit the functional relationship between the characteristic parameters of worn slip jaw height and the radial slip jaw gripping force/sliding friction coefficient, a predictive model was established for the variation in gripping performance of worn slip jaws with their height. Consequently, a testing and evaluation methodology for the gripping performance of worn slips in Snubbing Units has been established, providing a methodological framework for assessing the gripping capability of worn slips in Snubbing Units.

Keywords

Snubbing Units; Slip Heights; Quantitative Characterisation; Friction Coefficient; Clamping Performance.

1. Foreword

As the core component of the Snubbing Unit, the clamping performance of the clamp directly impacts the safety and efficiency of snubbing operations.[1-5]. Due to the lack of scientifically validated methods for assessing the clamping capacity of worn slip rods in field operations, the current precautionary approach to prevent accidents involves the premature replacement of worn slips, resulting in considerable material wastage. Present inspections of Snubbing Units predominantly utilize non-destructive testing techniques. Nevertheless, these methods are confined to identifying structural defects and cracks within the slip components and do not enable quantitative characterization of tooth wear patterns. As a result, evaluating the performance degradation of worn slip jaws during lifting operations remains a significant challenge.

Extensive research has been conducted by scholars both domestically and internationally on the structure of the Slip. Studies [6-8] have shown that Slip failure is caused by root fractures at the base of the teeth. The penetration depth of the Slip teeth into the tubing increases with load, whereas it gradually decreases as the number of teeth increases.The computational model

ISSN: 2688-8645

describing the contact force between the slip and tubing clarifies the underlying causes of stress concentration at the slip teeth, indicating that such stress concentration is the primary factor leading to non-uniform tubing damage and fracture [9-11]. Building on these findings, Lu Ming et al. [12] utilized a BP&NSGA-II finite element model to analyze the mechanical behavior during slip anchoring. In their research, key parameters—including slip inclination angle, internal cone angle, curvature radius, and pitch—were optimized with slip gripping performance as the evaluation metric. Furthermore, a matrix theory-based computational model for slip engagement force was developed [13], demonstrating a relationship between engagement force and tool angle during slip tooth machining. In addition, Tang Liping et al. [14-15] conducted optimization studies on design parameters such as drill pipe slip inclination angle, tooth height, and number of rows.

Tang Yang et al. [16-17] observed that as the number of teeth, pitch, or top angle of the slip jaws increased, the bending moment of the jaws grew while their anchoring performance diminished. They subsequently optimised the dimensional parameters of the slip jaws using an orthogonal experimental design. Ma Weiguo et al. [18] proposed a coupled structural optimisation methodology for slip gripper design, integrating finite element analysis, orthogonal testing, linear weighting, and MATLAB optimisation tools. They optimised parameters including groove width, position, and tooth crest width. Han Chuanjun et al. [19] employed slip line theory, combined with finite element analysis and experimental methods, to investigate contact stress distribution patterns on the tooth surface during clamping. Dong Xuecheng et al. [20] utilised finite element analysis and laboratory testing to explore the influence of parameters such as tooth front angle and tooth top radius on stress distribution, subsequently optimising the slip structure. Xu Jianning et al. [21] designed a novel biomimetic scaly tooth structure for the Slip profile, effectively improving the friction coefficient at the contact interface between the Slip and tubing. This optimised the stress distribution and bite mark characteristics on the tubing surface under Slip loading.

The aforementioned scholars primarily optimized the slip structure parameters through theoretical analysis, simulation calculations, and structural improvements, thereby enhancing clamping performance and improving stress distribution within the slip teeth. However, with respect to the wear of slip tooth height during operation, there remains an absence of analytical methods to evaluate the clamping capability of the slip in Snubbing Unit operations, particularly in a manner that correlates the wear characteristics of the slip teeth.

Building on this foundation, the present paper employs a die-cutting method to measure and characterize the height of slip teeth under various service conditions. A test platform has been developed to simulate the actual loading conditions of the slip teeth during Snubbing Unit operations, specifically for assessing the pipe-gripping performance of the slip teeth. Additionally, the study examines the relationship between radial gripping force and sliding friction of the pipe under distinct contact stresses, using grey-scale analysis to evaluate tubing clamping performance under simulated pressurized operating conditions. By integrating this with grey-scale image processing of color changes on pressure-sensitive paper under different contact stresses, the research explores variations in radial clamping force, sliding friction coefficient, and axial clamping force across slip teeth of varying heights. This approach elucidates the degradation mechanisms of clamping capability in worn slip jaws of Snubbing Units and provides methodological support for evaluating their tubing clamping performance.。

2. Materials and Methods

2.1. Test Materials

The on-site snubbing unit is of model DYJ11070DD. The tubing and slip plates originate from the Chuanqing Drilling rig. Both the tubing and slips have a diameter of 2 7/8″, with the tubing

ISSN: 2688-8645

wall thickness measuring 5 mm. Each slip plate consists of 18 horizontal rows and 4 vertical columns of slip teeth, totaling 72 teeth. Four slip plates together form a single integrated slip assembly. The specifications and parameters for the hydraulic slip seat, slip plates, and tubing of the Snubbing Unit are detailed in Table 1. Figure 1 depicts the specification parameters of the slip plates for the Snubbing Unit.

Table 1. Slip seat - Slip tooth plate specifications and parameters

Component	Project	Parameters
Slip Seat	**Cr(Slip rated load)**	**113t**
	Ts(Maximum lifting capacity of the hydraulic cylinder)	**110t**
	Pn(Rated working pressure)	**70MPa**
	Tp(Maximum downward pressure)	**75.7t**
Slip chewing plate	**Lc(Dental plate length)**	**168.71mm**
	Lk(Tooth plate width)	**38.12mm**
	Ld(Tooth width)	**8.14mm**
	α(Corner wrap)	**77.15°**

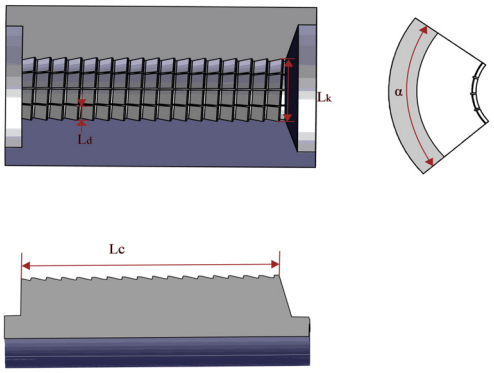

Fig 1. Schematic diagram of the structure of slip

2.2. Highly Quantitative Characterisation Method for Cavity Depth

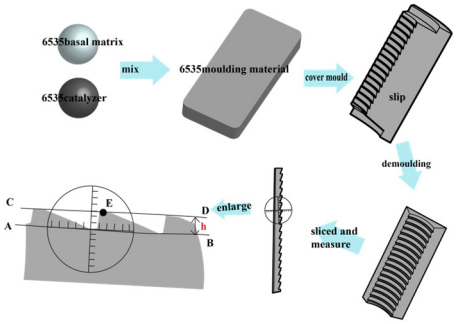

Fig 2. Schematic diagram and process of measuring the height of slip teeth using the die-cutting method

The height of the slip teeth is a critical determinant of the operational performance of the slip. This study employs the die-cutting detection method [22] to quantitatively assess the height of slip teeth. Figure 2 presents the workflow and principles of the die-cutting detection method for measuring slip tooth height. The measurement procedure is as follows: Equal volumes of 6535 base matrix (AFFINIS) and 6535 catalyst (AFFINIS) are combined. The resulting 6535 silicone rubber base impression material (AFFINIS) is applied to the slip denture plate where height measurement is required, filling the gaps between cusps. After curing, the material is demoulded and sliced into thin sections (1 mm thick). Measurements are carried out using a

ISSN: 2688-8645

floor-standing, fully automatic video measuring system (VMS-5040H). Using the tangent line AB at the base of the slip tooth as a reference, a parallel line CD is drawn through the apex point E of the slip tooth, and the height h is determined (as illustrated in Figure 2). This method allows for characterisation of slip tooth height after wear, providing essential data for examining how variations in slip tooth height affect the performance of slip-clamped tubing.

2.3. Radial Force Measurement Solution for Slip-Holding Oil Pipes

The operating principle of the DYJ11070DD pressure-operated hydraulic slip is illustrated in Figure 3. As the tubing's weight is applied, the slip teeth move along the wedge-shaped surface of the slip seat, resulting in the radial displacement of the slip body to clamp the tubing string. To understand how this clamping action affects the slip plate, it is essential to consider the stress analysis when the Snubbing Unit clamps the tubing and reaches a state of force equilibrium:

$$\begin{cases} F = G \\ F = \mu N \end{cases} \tag{1}$$

This paper uses pressure-sensitive paper to measure the radial clamping force N exerted by the pipe clamping jaws on the tubing. Before utilizing the pressure-sensitive paper to measure the radial force of the jaws, the color-developing stress of the paper was calibrated using an electronic universal testing machine (TSE105D) manufactured by Shenzhen Wantech Testing Equipment Co., Ltd. The calibration procedure is presented in Figure 4, with the steps detailed as follows:

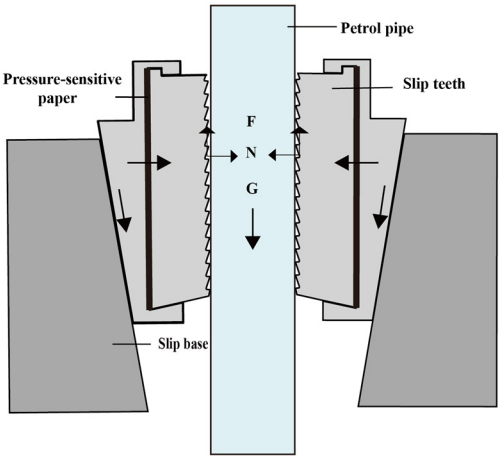

Fig 3. Schematic diagram of the principle of hydraulic slip clamping oil pipes under pressure

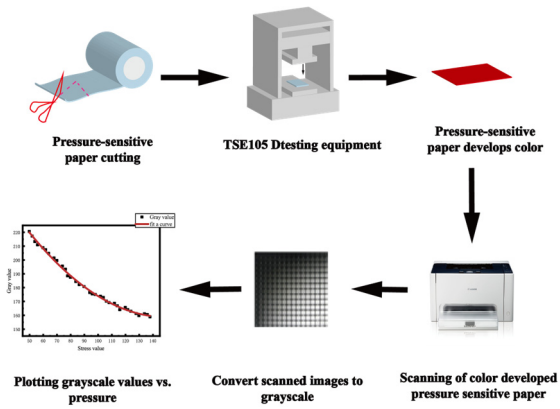

Fig 4. Pressure-sensitive paper calibration test procedure

ISSN: 2688-8645

Cut the pressure-sensitive paper into 20 mm × 20 mm squares. Place the paper on the test bench of the electronic universal testing machine (TSE105D), apply the initial load, and maintain the pressure for 2 minutes to allow color development in the paper under compression. For calibration, replace the paper and increase the load in predetermined increments, documenting each increment level. Repeat the test twice for each load level within the range of 1 MPa to 200 MPa. Digitize the pressure-sensitive paper using a scanner. Import the scanned image into MATLAB software, convert it to a grayscale image, and obtain the corresponding grayscale value for that stress level. Plot the pressure-sensitive curve with the grayscale value as the x-axis and stress as the y-axis.

Following the calibration experiments (after removing outliers), a scatter plot of pressure sensitivity against grey scale values was generated using Origin software, with stress plotted along the x-axis. Numerical fitting was conducted using the least squares method, as shown in Figure 4. This produced the following fitted equation describing the relationship between stress P and the grey scale value gr of the pressure-sensitive paper:

$$P = 5.3734 \times 10^3 \times \left(\frac{1}{gr}\right)^3 \tag{2}$$

Number the pressure-sensitive paper attached to the rear surface of the slip plate as illustrated in Figure 5. Determine the radial clamping force for the complete slip set using Formula (3). After testing, acquire the grey scale values of the corresponding numbered pressure-sensitive paper through a scanner. Insert these values into Formula (2) to compute the stress values. By combining these results with Formula (3), the radial clamping force for the entire slip set can be obtained.

$$N = \sum_{i=1}^{4} \sum_{j=1}^{12} P_{ij} S \tag{3}$$

In the formula, G represents the dead weight of the applied tubing, F denotes the frictional force generated by the slip jaws gripping the tubing, N signifies the radial gripping force exerted by the slip jaws on the tubing, μ indicates the coefficient of friction between the slip jaws and the tubing, and S denotes the area of the pressure-sensitive paper.

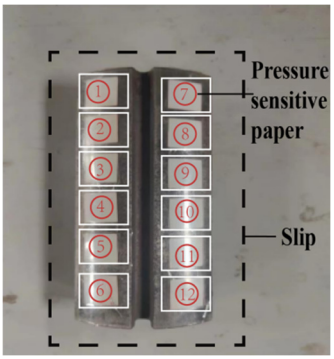

Fig 5. Pressure-sensitive paper sticker on the back of the slip

2.4. Performance Testing Protocol for Slip Clamp-Held Oil Pipes

This study employed a microcomputer-controlled electro-hydraulic servo pressure testing machine (WDYS-5000), manufactured by Changsha Yaxing CNC Technology Co., Ltd., to perform performance tests on pipe clamping using slips [23-24]. By machining a threaded connection plug at the bottom of the tubing, the machine's downward pressure rod transmits the applied load through the plug, converting it into tensile force on the tubing. This setup simulates the self-weight load of the tubing at different drilling depths. The principle of the

ISSN: 2688-8645

testing platform for evaluating slip grip performance under varying tubing string self-weights is shown in Figure 6.

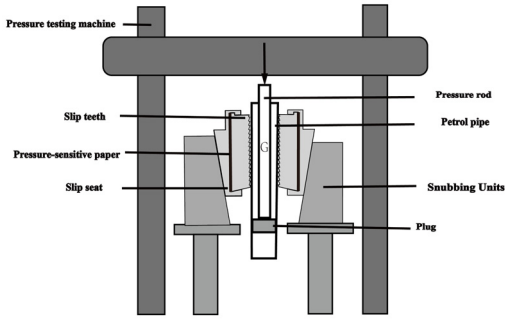

Fig 6. Slip clamp oil pipe performance test platform diagram

During field operations, if abnormal noises are detected from the slips, they should be replaced. However, this does not accurately indicate whether the slips have failed to grip the tubing. According to the tubing inspection standard [25] in the petroleum drilling and production industry, which specifies that 'the radial depth of the bite mark shall be less than 5% of the pipe wall thickness,' tubing is considered defective if the depth of the slip teeth penetration exceeds 5% of the wall thickness. In practice, it is not possible to observe or measure the depth of slip penetration into the tubing in real time, making this criterion impractical for assessing slip grip failure.

Therefore, a quantitative and visual criterion for evaluating slip grip failure on the tubing is necessary. This study uses real-time camera monitoring during gradient load testing. It records the displacement S of the pipe as it moves along the conical inner wall of the Snubbing Unit while clamped by the slip jaws. If this displacement increases steadily with the gradient load until the axial load exceeds Fm and is then followed by a sudden jump in displacement (recorded as Sm), causing the tubing to slip or fall, the slip is considered to have failed. The load Fm is subsequently defined as the maximum clamping capacity of the slip.

The test procedure is as follows: After installing the pressure-sensitive paper-lined slip plate into the Snubbing Unit, advance the assembled Snubbing Unit into the base of the pressure testing machine, as shown in Figure 6. The test loading gradient is set to 1T, with a pressure holding time of 1 minute. Increase the load to the maximum axial load Fm that the slip assembly can withstand (the ultimate load corresponds to the maximum downward tubing load of 75.7 tonnes), causing the tubing to slip or fall. A camera monitors the process in real time, measuring and recording the displacement S, as illustrated in Figure 7. After the test, measure the depth of the pipe bite marks and the grayscale value of the pressure-sensitive paper on the back of the slip. Using Formula 1 and Formula 2, the maximum radial clamping force N and the coefficient of sliding friction μ for this slip set can be calculated.

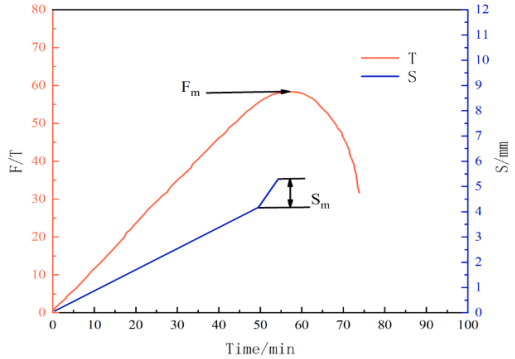

Fig 7. Schematic diagram of load and displacement changes during performance testing of slip clamp oil pipe

ISSN: 2688-8645

3. Results and Discussion

3.1. Height Characteristics of Various Slip Gauges

Figure 8 shows a box plot of eight sets of slip tooth height data obtained through the die-cut part dimension inspection method, using the five-number summary approach, with slip number on the x-axis and slip tooth height on the y-axis [26]. The black horizontal line represents the median slip height, while the orange horizontal line indicates the mean value. The box in the plot covers data points between the 25th and 75th percentiles of slip height within each group. The upper and lower whiskers correspond to the maximum and minimum slip height values, respectively. Observations showed slip heights ranging from 1.776 to 3.040 mm, with average slip heights varying between 2.296 and 2.921 mm. As slip wear increased, both the average and median slip heights decreased. Higher degrees of wear were associated with greater variability in slip height. Measuring slip heights across groups with differing wear levels provides data to analyze the variation patterns in clamping performance under different wear conditions.

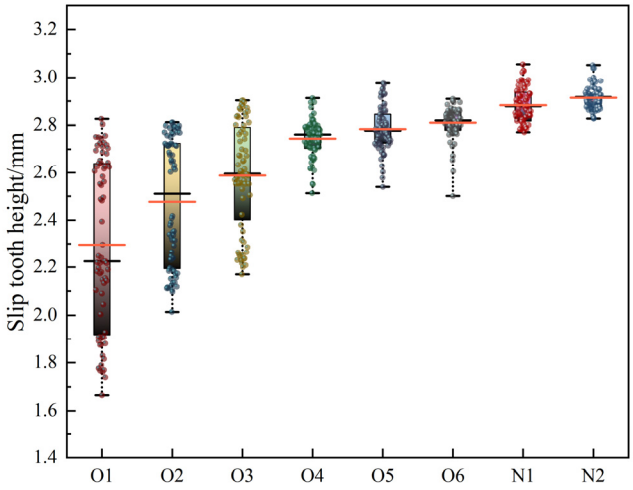

Fig 8. Slip tooth height characterisation data box diagram

3.2. Analysis of Variation Patterns in the Gripping Performance of Slip Assemblies under Various Wear Conditions

Performance measurement tests were conducted on eight sets of slip clamps. After testing, the bite marks on the pipes did not reach the depth required by the pipe failure standards of the petroleum drilling and production industry. Figure 9 presents the mapping relationship plots created by fitting the mean height of the slip clamp teeth against the radial clamping force and sliding friction coefficient using the least squares method. The corresponding equations are as follows:

$$N = -2.05354\times10^5 + 2.38285\times10^5 h - 9.1205\times10^4 h^2 + 1.1740\times10^4 h^3 \quad (4)$$

$$\mu = 0.60791 - 0.46078h + 0.10419h^2 \quad (5)$$

As shown in Figure 9, the height of the pressure-bearing slip teeth, the radial clamping force, and the coefficient of sliding friction between the slips and the tubing are all positively correlated. In other words, the taller the slip teeth, the deeper they penetrate under load, the greater the radial clamping force they generate, and the higher the coefficient of sliding friction between the slips and the tubing. After the slip teeth experience wear, the reduced height results in shallower penetration into the tubing. As a result, the radial clamping force exerted

ISSN: 2688-8645

by the slip teeth decreases, and the coefficient of sliding friction between the slips and the tubing is reduced, leading to a decline in the clamping performance of the slips.

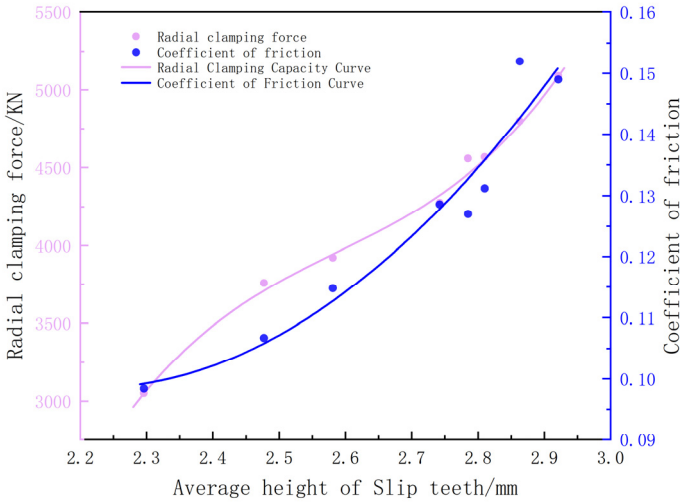

Fig 9. Map showing the relationship between radial clamping force, friction coefficient and average slip tooth height

3.3. Fitting and Validation of the Slip Clamping Capacity Prediction Model

Figure 10 presents the prediction model of the fifth-order polynomial function (Formula 6) for the Slip clamping force, fitted using the least squares method by integrating Equations (1), (4), and (5) based on the experimental results, as follows:

$$F = 1.2231\times10^{3}h^{5} - 9.5023\times10^{3}h^{4} + 7.3989\times10^{4}h^{3} - 1.886637\times10^{5}h^{2} + 1.543181\times10^{6}h - 1.24836\times10^{5} \quad (6)$$

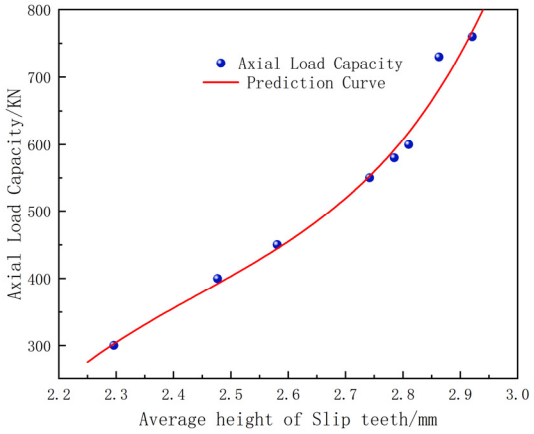

Fig 10. Slip clamping capacity mapping diagram

The height of the slip teeth is positively correlated with the slip's ability to grip the tubing. As the axial load increases, the slip teeth penetrate the tubing to their maximum depth, at which point the radial gripping force reaches its peak and the slip's capacity to secure the tubing is maximized. If the axial load continues to increase, the slip will fail to maintain its grip, resulting in slippage.

To validate the predictive model's accuracy and reliability, three additional sets of slip assemblies were tested, with average slip heights of 2.649 mm, 2.532 mm, and 2.321 mm, respectively. The results, shown in Figure 10b, indicate that the relative errors between the axial clamping force predicted by the model (Formula 6) and the experimentally measured axial clamping force were 5.4%, 7.2%, and 4.4%, respectively. All errors were within the engineering

ISSN: 2688-8645

tolerance of 10%, thereby confirming the model's accuracy and reliability. Based on these findings, it is recommended that any slip group with an average tooth height below 2.5 mm be mandatorily replaced to prevent potential safety incidents.

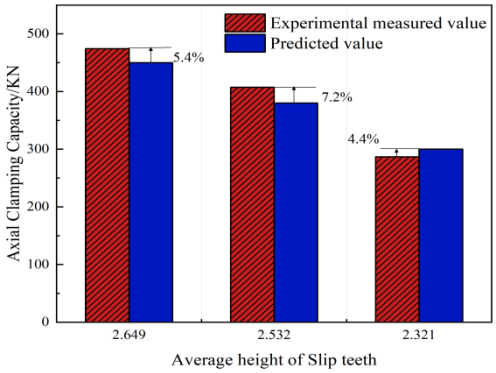

Fig 11. Prediction model validation results

4. Conclusion

1) For slip teeth that exhibit varying levels of wear in Snubbing Units, an effective method has been proposed to quantify wear depth using die-cut inspection. When combined with five-number summary statistics, this method allows for a quantitative characterization of slip teeth across different wear conditions within slip assemblies.

2) To address the actual loading conditions experienced when slip chocks grip tubing, a microcomputer-controlled electro-hydraulic servo pressure testing machine and slip chock jaw fixtures were utilized. A Snubbing Unit tooling fixture for slip jaws, incorporating image processing of pressure-sensitive paper gray-scale values under load, was employed. This innovation establishes a bench test apparatus and analytical methodology for simulating and evaluating the performance of slip jaw assemblies at various stages of wear when gripping tubing. A measurement criterion is proposed to assess the degradation in tubing grip performance under load, combining sudden axial pressure drops with tubing slippage.

3) The average height of the slips in the slip set used on site ranged from 2.921 mm to 2.296 mm. As the average slip height decreased from 2.921 mm to 2.296 mm, the radial clamping force followed a third-order polynomial decay pattern. $N = -2.05354\times10^{5} + 2.38285\times10^{5}h - 9.1205\times10^{4}h^{2} + 1.1740\times10^{4}h^{3}$; The coefficient of sliding friction decreases as the average height of the slip teeth decreases, following a second-order polynomial decay function. $\mu = 0.60791 - 0.46078h + 0.10419h^{2}$.

4) Based on the functional relationship F = N × μ for the axial load-bearing capacity of slip clamps, a predictive model has been developed to determine how the axial force applied by the teeth of slip clamps during snubbing operations changes with varying tooth height due to wear. $F = 1.2231\times10^{3}h^{5} - 9.5023\times10^{3}h^{4} + 7.3989\times10^{4}h^{3} - 1.886637\times10^{5}h^{2} + 1.543181\times10^{6}h - 1.24836\times10^{5}$, Based on the test platform for slip assemblies under varying wear conditions, the predictive model demonstrated a relative error of 7.2%, significantly below the engineering tolerance of 10%. Accordingly, an engineering recommendation was made to mandate replacement when the worn slip tooth height reaches a safety threshold of 2.5 mm. This provides a sound methodological foundation for evaluating the gripping performance of worn slips during Snubbing Unit operations.

References

[1] Judy Feder. Snubbing Unit Brings Middle East Well with Underground Blowout Under Control[J]. Journal of Petroleum Technology,2020, Vol.72(1): 66-67.

[2] Wang Wei. Technical Status and Application Analysis of Non-Pressurised Well Operations Equipment [J]. Petroleum Machinery, 2014, 42(10): 86-89.

[3] Zhang Dongping, Zhang Jian, Ji Fengjie. Technical Development of Pressure-Retaining Operation Equipment [J]. Petroleum Field Machinery, 2016, (08): 27-30.

[4] Zhao Guoqiang. Analysis of the Current Application Status of Hydraulic Slips [J]. Petroleum and Chemical Equipment, 2020, 23(11): 55–57.

[5] Hu Xuguang, Li Qian, Luo Yuan et al. Key Technologies and Prospects for Pressure-Retaining Operations in Gas Wells [J]. China Petroleum Exploration, 2023, 28(05): 135-144.

[6] Cai, MJ (Cai, Maojia), et al. Analysis of Interaction between HTHP Completion Packer's Slip and the Casing Wall[J]. APPLIED MATERIALS AND TECHNOLOGIES FOR MODERN MANUFACTURING, PTS 1-4, 2013, Vol.423-426: 866.

[7] Liu, Y (Liu, Yang), et al. Fracture failure analysis and research on slip of casing head(Article)[J]. Engineering Failure Analysis, 2019, Vol.97: 589-604.

[8] Song Chao, Nie Yunfei, Wu Zhonghua et al. Finite Element Analysis of the Slip Collar in Top Drive Running Rigs [J]. Journal of Beijing University of Chemical Technology (Natural Science Edition), 2016, 43(03): 85-90.

[9] Wang Lin, Ping Enshun, Li Nan, et al. Mechanical analysis of the setting process of degradable bridge plugs using the Slip method [J]. Petroleum Machinery, 2017, 45(12): 48-52. DOI: 10.16082/ j. cnki. issn. 1001-4578.2017.12.010.

[10] Zhang, H., Shu, C., Dou, Y. H., et al. Mechanical analysis of the interaction between wedge packer claws and tubing. Mechanical Design and Manufacturing Engineering, 2017, 46(10): 34-37.

[11] Lian, Z. H., Wan, Z. Y., Wu, Y. X., et al. Finite element analysis of the mechanical strength of tubing in ultra-deep well Slip suspension systems. Petroleum Machinery, 2023, 51(09): 1-8. DOI: 10. 16082/ j. cnki.issn.1001-4578.2023.09.001.

[12] Lu Ming, Liao Hualin, Wang Huajian, Liu Jiansheng, He Yuhang, Qu Fengtao, Niu Wenlong, Wang Yifan. Research on Prediction and Optimization Design Method of Slip Anchoring Performance Based on BP&NSGA-II. [J]. Front. Energy Res, 2022(10):907877.

[13] Han Feng, Gu Lei, Cui Xiaojie, et al. Research on the Mechanical Model of the Embedded Slip Tailpipe Hanger Seating System [J]. Petroleum Drilling Technology, 2015, 43(06): 103-107.

[14] Tang, LP (Tang, Liping), et al. Optimization Analysis on the Effects of Slip Insert Design on Drill Pipe Damage[J]. Journal of Failure Analysis and Prevention,2016, Vol.16(3): 384-390.

[15] Liping Tang, Baolin Guo, Marcin Kapitaniak, et al. Finite element analysis of drill pipe-slip system[J]. Journal of Petroleum Science and Engineering,2022, Vol.220: 111163.

[16] Tang Y, Sun P, Wang G, et al. Analysis of pressure-bearing performance and optimization of structural parameters of the slip in a compression packer. [J]. Sci Prog, 2020(103):1-19.

[17] Yang Tang, Jie Wang, Minghai Zhou,et al. Casing failure mechanism and slip anchoring optimization of the compression packer in the oil and gas well[J]. Proceedings of the Institution of Mechanical Engineers, Part E: Journal of Process Mechanical Engineering,2024, Vol.238(6): 2759-2769.

[18] Ma Weiguo, Shen Rufang, Zhao Guoqiang et al. Optimised Design of Hydraulic Slip Structure for Heavy-Load Non-Killing Operations [J]. Petroleum Machinery, 2020, 48(08): 69-76.

[19] Han Chuanjun, Peng Xuefeng, Li Lintao. Mechanical Behaviour of Packer Slip Anchoring and Analysis of High-Temperature and High-Pressure Testing [J]. Natural Gas Industry, 2020, 40(07): 76-82.

[20] Dong Xuecheng, Xiong Kerui, Wang Guorong et al. Structural Optimisation of Anti-Sticking Slip for Drilling Tools Based on Experimental and Numerical Simulation [J]. Journal of Southwest Petroleum University (Natural Science Edition), 2021, 43(01): 167-175.

[21] Xu Jianning, Deng Chong, Li Wanzhong. Micro-indentations and stability of hexagonal prismatic slip-shaped jaws in bionic packers [J]. Science and Technology and Engineering, 2022, 22 (15): 6075-6083.

ISSN: 2688-8645

[22] Yan Mengfei. Design of an Automatic Feeding and In-line Quality Inspection System for Laser Die-cutting Production Lines [D]. Nanjing Agricultural University, 2023.

[23] Wang Zifei, Li Jinbang, Xu Zhengrong, et al. Friction Test Machine with Dual-Paired Sliding-Rolling Pseudo-Bearing and Its Application [J/OL]. Journal of Tribology, 1-16 [2025-08-20]. https:// link. cnki. net/urlid/62.1095.O4.20250411.1423.004.

[24] Li Shuai, Jiang Cheng, Lou Wenjing, et al. Experimental observation of micro-pitting in bearing steel under oil-lubricated rolling contact conditions. Journal of Tribology (Chinese and English), 2025, 45(02): 231-241. DOI: 10.16078/j.tribology.2023284.

[25] Xu Xuesong, Miao Xin. Analysis and Validation of Bite Depth in Deep Well Tubing Held by Slip Clamps [J]. Equipment Maintenance Technology, 2023, (04): 23-26. DOI: 10.16648/j.cnki.1005-2917.2023.4.005.

[26] Wang Lijun, Wang Chengguang, Li Xiangyang, et al. Solving Dynamic Scheduling Problems in Distributed Heterogeneous Workshop Environments Using Multi-Agent Deep Reinforcement Learning [J/OL]. Computer Integrated Manufacturing Systems, 1-19 [2025-08-20]. https://doi. org/ 10. 13196/j.cims.2024.0602.